Properties of Functionally Graded Coating of Al_2O_3/ZrO_2/HAP on SS 316L

Rana Afif Majed Anaee[1]

Abstract—This study describes the synthesis of ZrO_2/HAP and Al_2O_3/ZrO_2/HAP functionally graded coating on SS 316L as bioimplant by atomization and compared them with uncoated and coated samples with HAP alone. A suitable suspension that was based on ethanol was applied for coatings. AFM analysis used to characterize the coated surfaces and measure the roughness which indicates the increasing the roughness of ZrO_2/HAP and Al_2O_3/ZrO_2/HAP compared with HAP coating which provide the adhesion between the bioimplant and tissue. Corrosion measurements carried out to estimate the properties of coated surfaces and showed that functionally graded coating gave properties better than HAP coating through protection efficiencies and porosity percentages. Cyclic polarization measurements also confirm the above results.

Index Terms—Functionally graded coating; Atomization; SS 316L; Hydroxyaptite.

1 Introduction

Functionally graded calcium phosphate coatings have the potential to meet the increasing protection efficiency of bioimplants. It also involves the synergies of two types of calcium phosphates, namely, α-tricalcium phosphate and HA, to form the FGM. Hydroxyapatite $Ca_{10}(PO_4)_6(OH)_2$ (HAP) is the vital constituent present in bones and teeth. HAP is the most versatile material used for implantation purposes owing to their similarity with natural bone mineral and its ability to bond to bone [1-3]. Many studies highlighted HAP coating using different methods to coating [4-11]

In this study, HAP has been prepared and characterized to use as coating of 100wt%HAP and as functionally graded coating with zirconia and mixture of alumina and zirconia. Coatings were applied by atomization process using airbrush with nitrogen gas. Corrosion test was achieved by Potentiostat in human body fluid at pH=7.4 and 37°C to estimate corrosion parameters and calculate protection efficiency and porosity percentage.

2 Materials and Methods

SS 316L specimens were used to test the corrosion for uncoated and coated samples with dimension of 10×10×3 mm. Ringer's solution tablets were used to prepare simulated human body fluid. HAP prepared according to schematic diagram as shown in Fig. (1), with particle size 0.931 µm. Alumina and Zirconia with particle size 0.896 and 0.441 µm respectively which tested by China Chengdu Jingxin powder analysis instrument.

Emulsions prepared for coating process by dissolving 0.5g of coating powder in 25ml ethanol (purity 99.99%). Ultrasonic and magnetic stirring achieved for 20 min. of each method. Airbrush with nitrogen gas used to spray the emulsion on heated specimens about 100+5°C using hotplate.

• [1]*Rana Afif Majed Anaee: Assistant Prof. Dr. at Materials Eng. Dep.- University of Technology/ Iraq-Baghdad, E-mail: dr.rana_afif@yahoo.com , dr.rana.a.anaee@uotechnology.edu.iq*

The distance between the nozzle and metallic surfaces was about 5 cm. By above procedure, three types of coatings were get include 100wt% HAP, 40wt%ZrO_2/60wt%HAP, and 30wt%Al_2O_3/30wt%ZrO_2/40wt%HAP.

Corrosion measurements tested to estimate the electrochemical behavior of uncoated and coated SS 316L samples using standard cell with three electrodes; working, auxiliary and reference. Protection efficiencies and porosities were calculated using certain formulas.

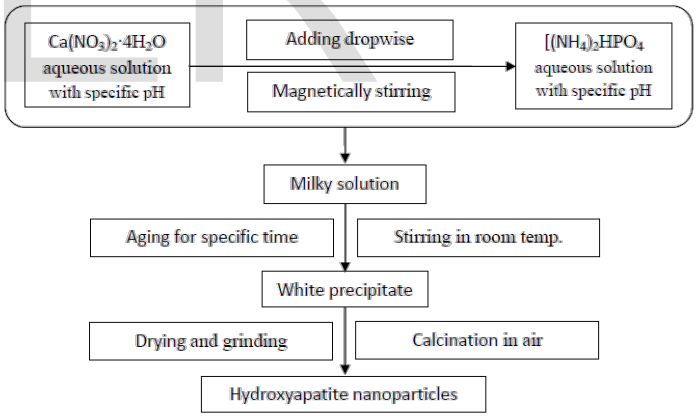

Figure (1) The flowchart of the chemical precipitation method used to prepare hydroxyapatite.

3 Results and Discussion

3.1 Characterization of Prepared HAP and Coated Surfaces

The prepared HAP characterized by XRD as shown in Figure (2) and the data are listed in Table (1) to conform the structure of HAP. FTIR with KBr disc was used to identify the prepared HAP as shown in Figure (3) with main peaks. The characteristic peaks appeared at 1048 cm^{-1} and 564.09 cm^{-1} are assigned to the phosphate groups of HAP. The broad stretching band at 3443.18 cm^{-1} and 603.11 cm^{-1} are assigned to the stretching and bending vibration of OH^- groups of HAP, respectively.

Atomic force microscopy was performed to display the surface topography of un-coated and coated metal surfaces. Figures (4) to (7) display the 2D and 3D images of coated surfaces for uncoated specimen and coated others with 100%HAP, 40%ZrO_2/60%HAP and 30%Al_2O_3/30%ZrO_2/40%HAP respectively. These images indicate the distribution of coating particles on SS 316L surface. The roughness values can be estimated from AFM inspection. The roughness of coated surfaces by HAP, ZrO_2/HAP, and Al_2O_3/ZrO_2/HAP are 1.09, 1.32, and 7.48 nm respectively which they support the interaction between the bioimplant and tissue better than with uncoated surface which has roughness 0.587 nm.

Table (1): XRD analysis for prepared hydroxyapatite according to JCPDS.

Card No.	Sys	$2\theta_s$	$2\theta_m$	I_s	I_m	a	c
24-0033	hexagonal	25.879	26.060	42	54.9	9.432	6.881
		31.739	31.997	100	100		
		32.865	32.786	55	75.1		

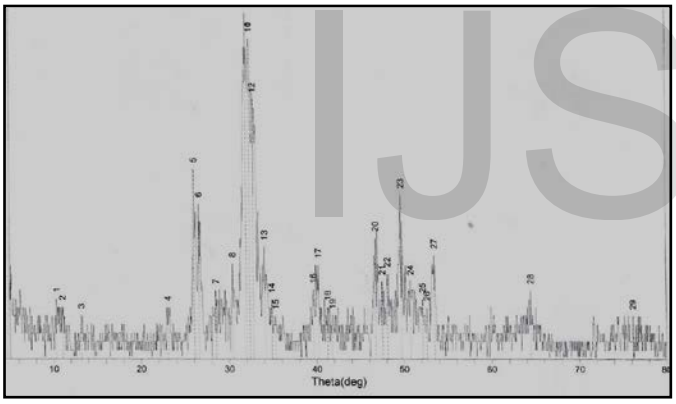

Figure (2) XRD of prepared HAP.

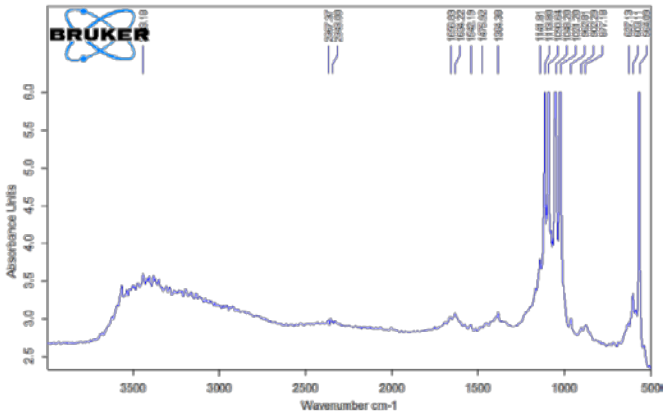

Figure (3) FTIR spectrum of HAP.

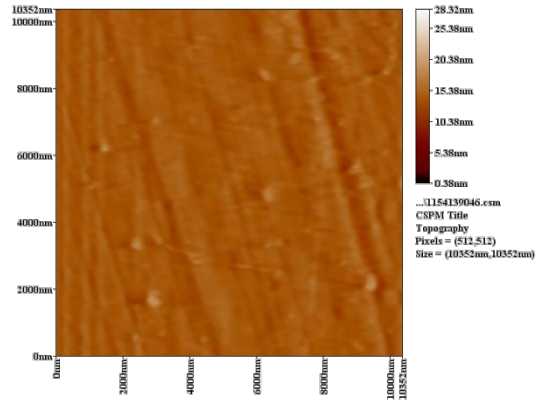

2D

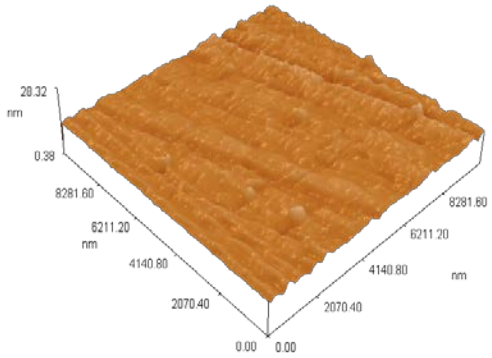

3D

Figure (4) AFM images of the surface of as polished SS 316L.

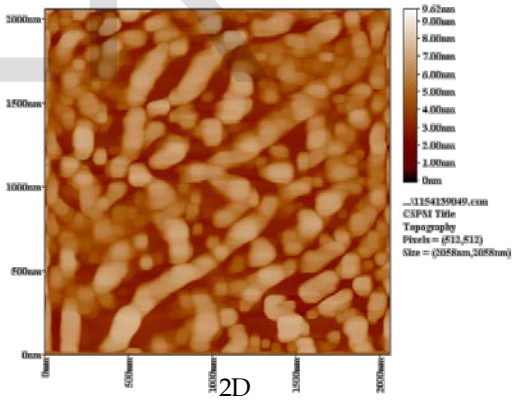

2D

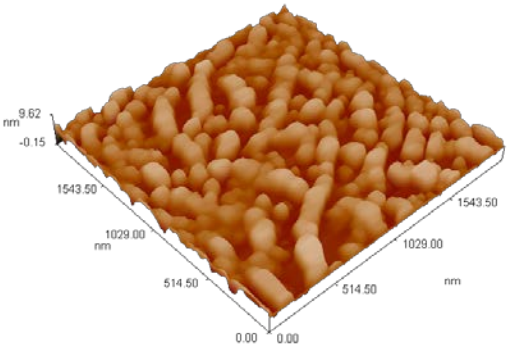

3D

Figure (5) AFM images of the coated surface with 100%HAP.

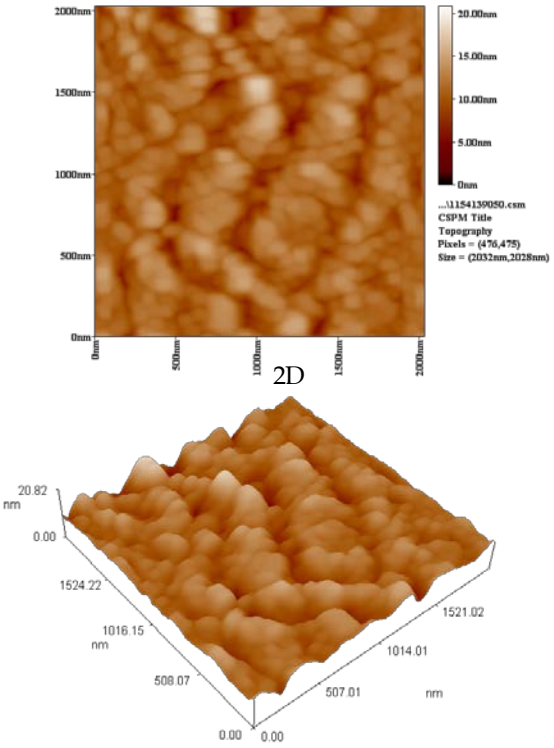

Figure (6) AFM images of the coated surface with 40%ZrO_2/60%HAP.

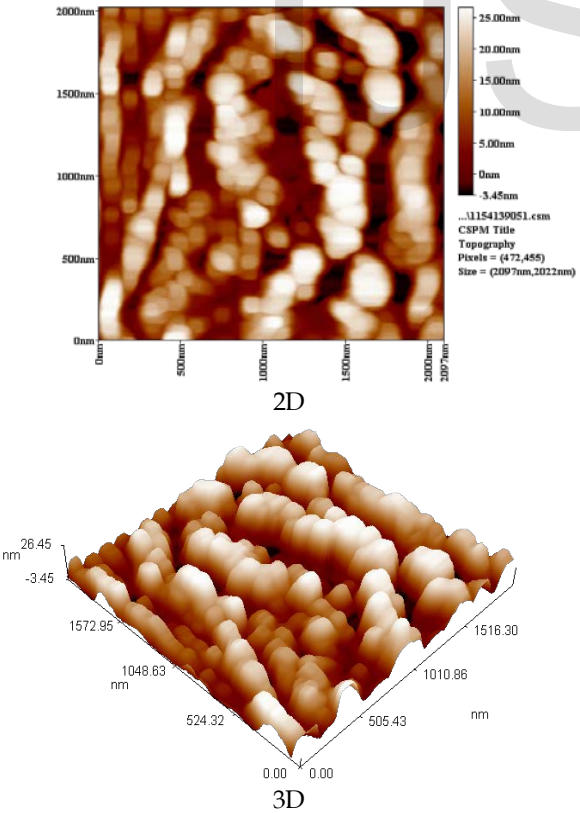

Figure (7) AFM images of the coated surface with 30%ZrO_2/30%Al_2O_3/40%HAP.

3.2 Electrochemical Behavior

Figure (8) shows the electrochemical behavior of polished SS 316L and coated specimens in human body fluid at 37°C and pH=7.4. The data of corrosion indicate that corrosion potential (Ecorr) became more noble after coating and we obtained less corrosion current densities as listed in Table (2).

This means that the dissolution of metals was decreased after coatings at anode according to the following reaction:

$$M \rightarrow M^{n+} + ne \quad (1)$$

While at cathode, the reduction of oxygen takes place to consume the electrons as follow:

$$O_2 + 2e + 2H_2O \rightarrow 4OH^- \quad (2)$$

The current densities (i_{corr}) can be used to calculate protection efficiencies PE% using the following formula:

$$PE\% = \left(1 - \frac{i_{corr,coated}}{i_{corr,uncoated}}\right) \times 100 \quad (3)$$

The data of PE% which are listed in Table (2) indicate that the coating by ZrO_2/HAP and Al_2O_3/ZrO_2/HAP gave PE better than coating with HAP alone.

The porosity percentage (PP%) can be calculated using the following equation:

$$PP\% = \frac{R_{P_{uncoated}}}{R_{P_{coated}}} 10^{\frac{-\Delta E_{corr}}{b_a}} * 100 \quad (4)$$

where R_p,uncoated and R_p,coated are the polarization resistances of the uncoated coated samples respectively, ΔE_{corr} is the corrosion potential difference between them, and ba is the anodic Tafel slop of the uncoated sample.

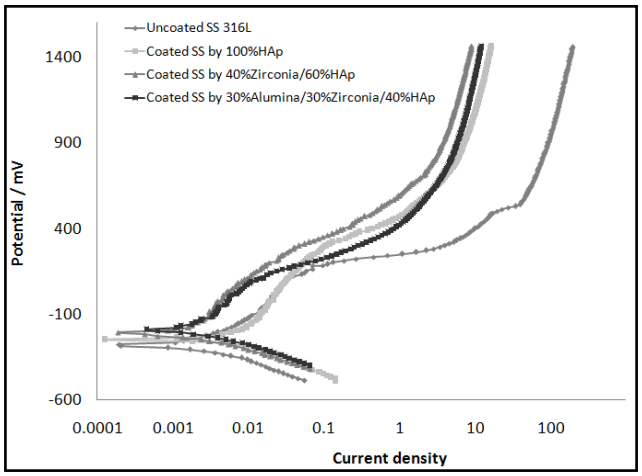

Figure (8) Electrochemical behavior of uncoated and coated SS 316L in Ringer's solution at 37°C.

Table (2): Electrochemical parameters for uncoated and coated SS 316L.

Coating type	E_{corr}/ *mV*	i_{corr}/ *μA.cm*$^{-2}$	$-b_c$/ *mV.dec*$^{-1}$	b_a/ *mV.dec*$^{-1}$	*PE/ %*	*PP/ %*
Uncoated SS	-278.1	2.68	159.9	268.9	--	---
HAP	-250.0	2.53	70.4	115.2	5.60	214.58
ZrO_2/HAP	-215.5	1.33	105.7	308.5	50.37	62.51
Al_2O_3/ZrO_2/HAP	-190.9	1.13	90.2	163.1	57.84	71.89

The data in Table (2) indicate that the ZrO_2/HAP coating gave the lowest porosity percentage of all three coatings, i.e., this coating decreases the ingress of ions through it.

3.3 Cyclic polarization behavior

This test is important tool to estimate the chance of occurrence pitting corrosion. Figures (9) and (10) show the cyclic polarization curves of uncoated and coated SS 316L specimens respectively. The coatings shifted the anodic curves toward passive region compared with uncoated sample. Also the difference between breakdown potential and repassivation potential for uncoated sample is larger than these for coated samples. Table (3) indicates the data of cyclic polarization. In spite of the coated sample with HAP gave the breakdown potential Eb more noble than other coated samples, the coating with Al_2O_3/ZrO_2/HAP gave the highest value of pitting potential Epit. The later result means that functionally graded HAP with alumina and zirconia give the best pitting resistance for SS 316L in human body fluid.

Table (3): The data of cyclic polarization curves.

Coating type	$+E_b$	$-E_{pit}$
Uncoated SS	22	357
HAP	208	79
ZrO_2/HAP	69	59
Al_2O_3/ZrO_2/HAP	109	40

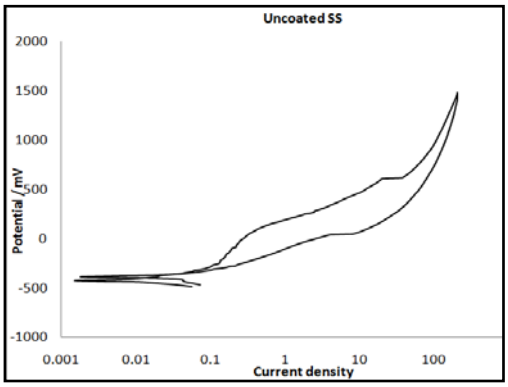

Figure (9) Cyclic polarization of uncoated SS 316L in Ringer's solution at 37°C.

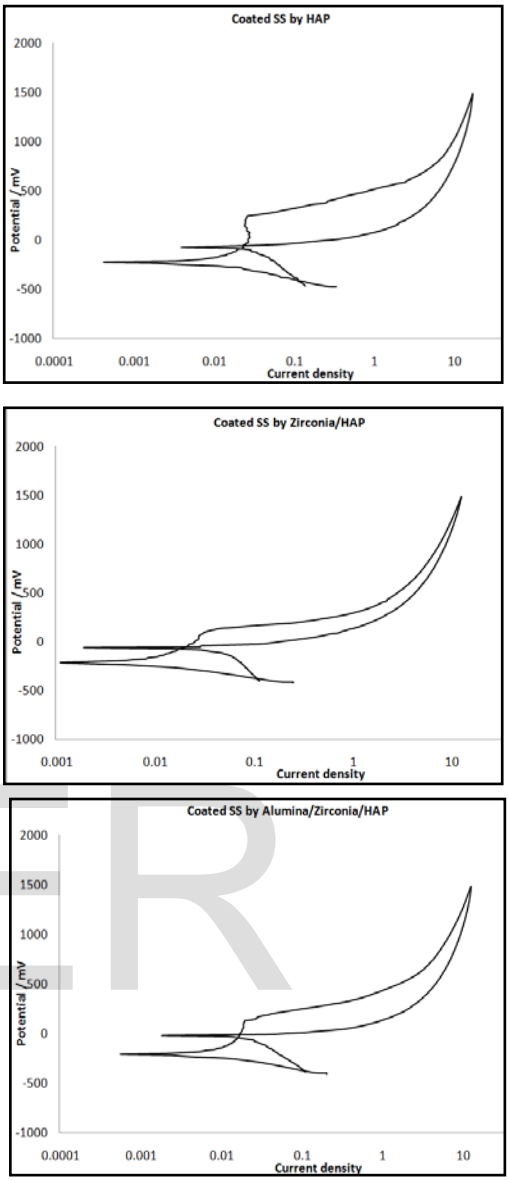

Figure (10) Cyclic polarization of coated specimens in Ringer's solution at 37oC.

4 Conclusion

The functionally graded coatings may be gave the results better than the coating of one component. In this work, the coating of ZrO2/HAP and Al2O3/ZrO2/HAP on SS 316L gave better results than the coating by HAP alone. AFM tests used to characterize the coated surface in addition to calculate the roughness which indicate that the coated surfaces had roughness more than for uncoated surface which help to formation some interaction between the implant and tissue after implantation. Corrosion measurements achieved to estimate protection efficiencies of coated surfaces in addition to calculate porosity percentages, these data indicated the better efficiency for coupled materials than the HAP alone. Also, the results of cyclic polarization were good agreement with the other tests.

REFERENCES

[1] Khor K A,WangY, Functionally Graded Coatings for Biomedical Applications. Surface Modification Technologies on CD (ASM International), 2001.

[2] Von RecumA F, Handbook of biomaterials evaluation – Scientific, technical and clinical testing of implant materials 2nd edn (Philadelphia: Taylor & Francis), 1999.

[3] Lin J H C, Kuo K H, Ding S J, Ju C P., Surface reaction of stoichiometric and calcium deficient hydroxyapatite in simulated body fluid. J. Mater. Sci. Mater. Med. Vol.12, pp.731–741, 2001.

[4] Miguel Manso, Carmen JimeHnez, Carmen Morant, Pilar Herrero and JMMartmHnez-Duart, "Electrodeposition of hydroxyapatite coatings in basic conditions", Biomaterials, Vol.21, pp.1755-1761, 2000.

[5] Yong-Mu Lim, Kyu-Seog Hwang and Yeong-Joon Park, "Sol-Gel Derived Functionally Graded TiO_2/HAP Films on Ti-6Al-4V Implants", Journal of Sol-Gel Science and Technology Vol.21, pp. 123–128, 2001.

[6] Dongxia Liu, Keith Savino, Matthew Z. Yates, "Coating of hydroxyapatite films on metal substrates by seeded hydrothermal deposition", Surface & Coatings Technology, Vol.205, pp.3975–3986, 2001.

[7] Zude Feng, Qishen SU and Zuochen LI, "Electrophoretic deposition of hydroxyapatite coating", J. Mater. Sci. Technol., Vol.19, No.1, pp.30-32, 2003.

[8] M. Saremi and B. Mottaghi Golshan, "Electrodeposition of nano size hydroxyapatite coating on Ti alloy", Iranian Journal of Materials Science and Engineering, Vol. 3, No. 3 and 4, Summer and Autumn 2006.

[9] Beatrice Plesingerova, Gabriel Sueik, Martin Maryska, Diana Horkavcova, "Hydroxyapatite coatings deposited from alcohol suspensions by electrophoretic deposition on titanium substrate", Ceramics – Silikáty, Vol.51, No.1, pp.15-23, 2007.

[10] Marija Mihailovic, Aleksandra Patarici, Zvonko Gulisija, Djordje Veljovic and Djordje Janackovic, "Electrophoretically deposited nanosized hydroxyapatite coatings on 316L stainless steel for orthopaedic implants", Chemical Industry & Chemical Engineering Quarterly, Vol.17, No. 1, pp.45−52, 2011.

[11] V Ozhukil Kollatha, Q Chenc, R Closset, J Luytena, K Trainab, S Mullensa, A R Boccaccinic, R Cloots, "AC vs. DC Electrophoretic Deposition of Hydroxyapatite on Titanium", J. Eur. Ceram. Soc. (2013), http://dx.doi.org/10.1016/j.jeurceramsoc.2013.04.030